Growth of ZnO Nanostructures with Different Morphologies by Using Hydrothermal Technique

Yanhong Tong,[†,‡,§] Yichun Liu,*[,†] Lin Dong,[||] Dongxu Zhao,[‡] Jiying Zhang,[‡] Youming Lu,[‡] Dezhen Shen,[‡] and Xiwu Fan[‡]

Center for Advanced Optoelectronic Functional Material Research, Northeast Normal University, Changchun 130024, People's Republic of China, Key Laboratory of Excited-State Process, Changchun Institute of Optics, Fine Mechanics and Physics, Chinese Academy of Sciences, Changchun 130033, People's Republic of China, Graduate School of Chinese Academy of Sciences, Beijing 100039, People's Republic of China, and School of Materials Science and Engineering, Zhengzhou University, Zhengzhou 450052, People's Republic of China

Received: May 29, 2006; In Final Form: July 24, 2006

ZnO nanostructures, including nanotowers, nanovolcanoes, nanorods, nanotubes, and nanoflowers, have been grown by using the hydrothermal technique. Most of the ZnO nanostructures show the perfect hexagonal cross section and well-faceted top and side surfaces. The basic chemistry and growth mechanism are discussed. By increasing the reaction time, the volcano-like and tube-like ZnO structures were formed due to the Ostwald ripening process and the selective adsorption of the complexes. By using the seed layer, the dense-arrayed, regular oriented ZnO nanorods were obtained due to the decreased nucleation barrier and the abundant interfaces as well as the increasing surface roughness.

Introduction

ZnO has a wide and direct band gap of 3.37 eV at room temperature with the large exciton binding energy 60 meV, which makes it a promising candidate for high-efficient, ultraviolet-light-emitting diodes (LEDs) and ultraviolet laser diodes (LDs). Owing to its noncentrosymmetric structure, ZnO is well-known as a piezoelectric material in surface acoustic wave (SAW) devices for delay lines, filters, resonators in wireless communication, and signal processing.[1] ZnO is also one of the promising materials for applications in transparent-conducting electrodes, catalysts, sensors, detectors, and flat-panel displays. Recently, the ferromagnetic behavior with a Curie temperature (T_c) value above room temperature in Mn-doped ZnO has been theoretically predicted.[2]

On the basis of the remarkable physical properties and the versatile applications of the ZnO material, a large effort has been focused on the synthesis, characteristics, device fabrication, and performance improvement of the ZnO nanostructures for semiconductor device miniaturization.[3,4] It is expected that the properties of the ZnO nanostructures can be well adjusted by size and shape. Currently, the growth mechanism and controlled crystalline morphology of the nanostructures still remain a significant challenge. A number of methods have been developed to fabricate ZnO nanostructures. For example, the anodic alumina membrane (AAM) has been used as the template to grow the well-defined one-dimensional (1D) ZnO nanostructures;[5] however, the polycrystalline ZnO nanostructures with the rough surfaces are generally obtained. The vapor transport process, mainly including the catalyst-free vapor−solid (VS) process and the catalyst-assisted vapor−liquid−solid (VLS) process, is a simple and conventional method to obtain a rich variety of the single-crystalline ZnO nanostructures.[3] However, a weak temperature gradient in the deposition region often results in the remarkable change in the shapes and the sizes,[6,7] which is not appropriate for large-scale production. Recently, the solution chemical route has become a promising option due to its mildness, simplicity, low cost, and high efficiency.

Currently, many groups have used the zinc nitrate and hexamethylenetetramine (HMT) aqueous solutions to fabricate ZnO nanostructures because only the two reactants are needed, which simplifies the experimental process.[8,9] The influence of some synthesis parameters on the morphology of ZnO nanostructures has been studied. For example, Vayssieres et al. have reported that the size of the ZnO nanostructures was decreased and the aspect ratio was increased with the decrease in the concentration of the reaction solutions.[10,11] Reaction time in the chemical solution reaction is another important parameter reflecting the thermodynamics and/or kinetics processes because of its close relation to the change of concentration and reaction rate in the reaction process.[12] However, most of the papers gave only the morphology changes with the increased reaction time. The reactive process and growth mechanism versus reaction time was not considered in depth. In addition, a large number of papers have reported the ZnO nanowire/nanorod arrays prepared by using seed layers as substrates since Yang et al. obtained the ultraviolet lasing of the ZnO nanowire arrays in 2001.[13,14] The ZnO nanowire/nanorod arrays, because of good stability and excellent and versatile properties in ZnO material, will possibly act as the basic building blocks for the nanoscale optoelectronic and piezoelectric devices.[15,16] However, most papers did not discuss the basic growth process and the role of seeds, but presented only the morphology of obtained ZnO nanowire/nanorod arrays,[17] which is disadvantageous to further adjust the morphology and size of ZnO nanostructures for

* Author to whom correspondence should be addressed. Tel: +86-431-5099168. Fax: +86-431-5684009. E-mail: ycliu@nenu.edu.cn.

[†] Center for Advanced Optoelectronic Functional Material Research, Northeast Normal University.

[‡] Key Laboratory of Excited-State Process, Changchun Institute of Optics, Fine Mechanics and Physics, Chinese Academy of Sciences.

[§] Graduate School of Chinese Academy of Sciences.

[||] School of Materials Science and Engineering, Zhengzhou University.

10.1021/jp063312i CCC: $33.50
Published on Web 09/19/2006

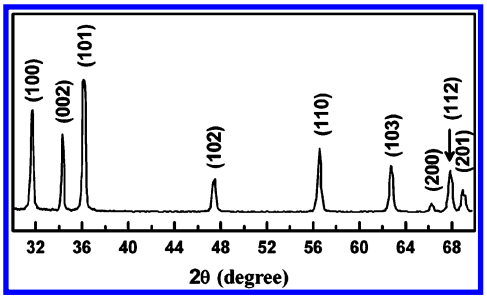

Figure 1. XRD pattern of the obtained ZnO powder collected in the solution.

practical applications. In this paper, we fabricated different ZnO nanostructures by the hydrothermal technique. To address the basic chemistry and growth process, the effect of the reaction time and seed layer on the morphology and size of ZnO nanostructures was studied under the condition of some fixed fundamental parameters, such as temperature and concentration.

Experimental Section

All chemicals were purchased from Beijing Chemical Reagent Corp. ITO, Si, ZnO-seed-coated Si, and ZnO-seed-coated ITO wafers were used as substrates. The ZnO seed layers were formed by electron beam evaporation. In a typical experiment, the reaction solution was prepared by mixing 0.05 mol/L zinc nitrate and 0.05 mol/L HMT aqueous solutions in a Teflon vessel. The substrates were vertically immersed into the reaction solution. The reaction temperature was kept at 90 °C. The reaction time changed from 0.5 to 6 h. Subsequently, the substrates were washed with deionized water and dried in air. At the same time, the white precipitate in the reaction solution was collected, centrifuged, washed using deionized water, and dried at 60 °C in air. The fabrication process for the tubular structure has been reported in detail in previous work.[18] The first-step reaction time for ZnO nanotubes was 3 h, and the second-step time was ~4 days. The reproducible ZnO nanostructures, including nanotowers, nanovolcanoes, nanorods, nanotubes, and nanoflowers, were obtained according to the reaction time and the seed.

The morphology of the products was observed by field-emission scanning electron microscopy (FESEM, Hitachi S-4800). The structural characterization was analyzed by X-ray diffraction (XRD; Rigaku D/max-rA) spectra with the Cu Kα line of 1.54 Å. The surface morphology of the thin films was investigated by atomic force microscopy (AFM, Di 3100s) images in the tapping mode. The root-mean-square roughness of the surface was obtained using the software provided by the instrument.

Results and Discussion

Structure and Morphology. All obtained powders show similar XRD patterns. A representative XRD spectrum of the ZnO powder is shown in Figure 1. All diffraction peaks can be indexed to hexagonal wurtzite ZnO, and no diffraction peaks of any other minerals are detected. The ZnO nanorods grown on ZnO-seed-coated Si and ITO substrates show the preferred (002) orientation (Figure 3e), indicating that the nanorods grow along the *c*-axis direction.

Figures 2 and 3 show the SEM images of the ZnO nanostructures. The tower-like, volcano-like, rod-like, tube-like, and flower-like ZnO nanostructures can be obtained in different conditions. The middle widths of the ZnO nanostructures range from several hundreds of nanometers to several micrometers, and the lengths range from 0.6 to 10 μm. The SEM images clearly reveal the well-faceted top and side surfaces with a hexagonal cross section for most of nanostructures.

HMT. Generally, ammonia or ammonium salts are introduced to the hydrothermal process because of the key atom nitrogen. The lone-pair electrons on nitrogen can coordinate the empty orbits of metal ions, generating metal−ammonium complexes. These complexes can form certain special structural units to modify, promote, and even direct the formation of versatile nanostructures. Hence, ammonia and ammonium salts are generally used as template solvents. Here, we select HMT as one of reactants. HMT can hydrolyze and decrease the concentration of H^+ ions for the nucleation and growth of ZnO nanostructures, as will be discussed below. Additionally, HMT is a well-known tetradentate ligand and tends to bind metal ions in different coordination modes including the monodentate and μ_n-bridging modes.[19] At the same time, the Zn^{2+} ion possesses strong polarity and deformability. Therefore, there is a strong combination between HMT and Zn^{2+} ions, and there they generate a large amount of Zn^{2+} amino complexes in solution. Our previous results have shown that Zn^{2+} amino complexes adsorb mainly on the side surfaces to facilitate the growth of 1D nanostructures and slow the dissolution of the side walls.[18] This is a key point for the formation of the volcano-like and tube-like ZnO nanostructures.

Basic Chemistry. In the current experiment, the reaction system maintains the weak acid condition and the pH value of the solution is ~5.5. The reaction processes in the system can be expressed by the following equations:

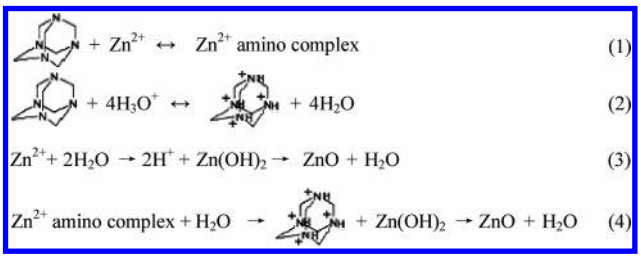

When HMT and zinc nitrate aqueous solutions were mixed at room temperature, the chemical equilibrium in eq 1 shifts to the right, and hence a large number of Zn^{2+} amino complexes were produced in the solution. In the hydrothermal condition, the equilibrium in eq 1 shifts to the left and the equilibrium in eq 2 shifts to the right, respectively, corresponding to thermolysis of Zn^{2+} amino complexes and the hydrolysis of HMT. The concentration of H^+ ions is decreased. This will facilitate the further hydrolysis of Zn^{2+} ions, that is, causing the chemical equilibrium in eq 3 to shift to the right. Additionally, a part of Zn^{2+} amino complexes will be directly hydrolyzed, and ZnO can be formed, as shown in eq 4.

Growth Mechanism. Most products show an uneven width change from the bottom of the single nanostructure to the top (tower-like structures). Wang et al. obtained similar ZnO nanostructures by mixing zinc nitrate, thiourea, and ammonium chloride aqueous solutions at 95 °C.[20] They proposed that the tower-like structure was produced by the layer−layer stacking of the ZnO nanosheets. In our experiments, with the increase of the reaction time from 1 to 3 h, as shown in Figure 2, parts c and f, both the widths and the lengths of the ZnO nanostructures increase, which indicates the transversal and longitudinal growth of the single nanostructure with the time. Therefore, the different growth pattern should be considered.

This uneven width change along the length for the single nanostructure may be related to the anisotropy of the ZnO material. The crystal planes which have higher surface energy

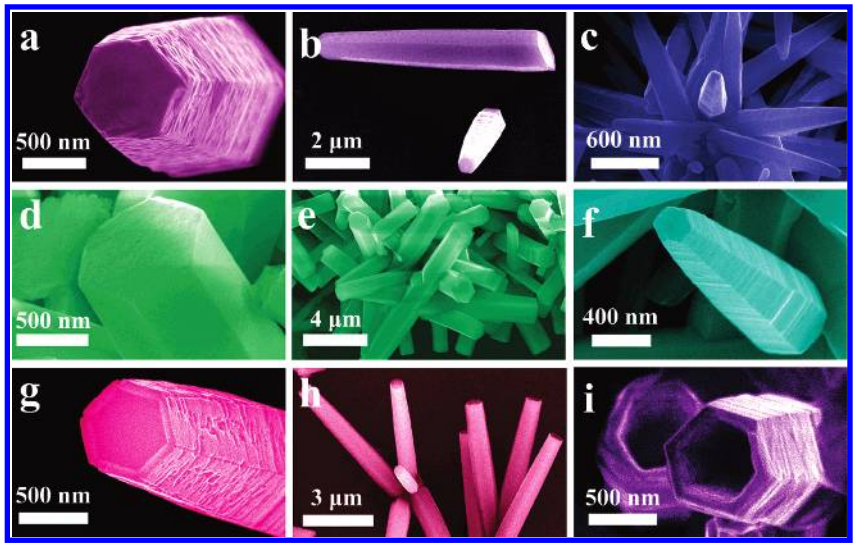

Figure 2. SEM images of ZnO nanostructures: (a,b) on ITO substrate for 3 h, (d,e) on Si substrate for 3 h, (g,h) on Si substrate for 6 h; (c) powder for 0.5 h, (f) powder for 3 h, (i) powder for 3 h + 4 days;

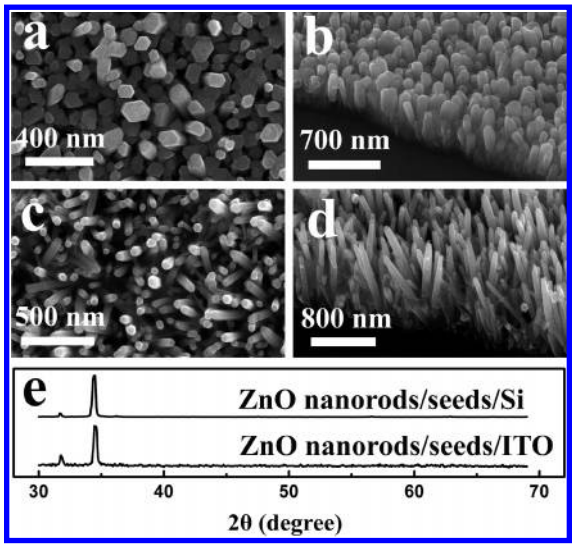

Figure 3. SEM images of ZnO nanostructures grown on (a,b) ZnO-seed-coated Si substrate, and (c,d) ZnO-seed-coated ITO substrate. (e) XRD spectra of ZnO nanorod arrays grown on Si and ITO substrates, respectively.

possess faster growth velocity. Because of the different surface energy, the growth velocity of the {0001} planes is higher than that of the {1000} planes. As a result, when different crystal planes grow at different velocities, those surfaces with the faster growth velocities ({0001} planes) will continually decrease their area and the surfaces with slower growth velocities ({1000} planes) will gradually dominate the morphology of crystal; this results in the formation of the 1D structure with the uneven width along its length. In fact, with the growth process, the length of the nanostructures increases, while the top area decreases gradually. This growth pattern will produce a number of steps on the side surfaces, resulting in the increase in both the surface/interface defects and the system energy in the ZnO nanostructures. Therefore, the growth pattern of ZnO nanotowers is not dominated by a thermodynamic process but by a kinetic process.

Reaction Time. Figure 2, parts c and f, respectively, correspond to the ZnO powders obtained by 1- and 3-h hydrothermal reactions. Figure 2i is the ZnO powder obtained by further reaction after the hydrothermal reaction for 3 h. When the reaction time is 1 h, the middle width of the obtained ZnO nanotowers (Figure 2c) is ~200 nm and the length is ~1 μm. When the reaction time increases to 3 h, the middle width increases to ~500 nm and the length increases to ~1.5 μm (Figure 2f). If the reaction time continues to increase, the single nanotower will be dissolved (Figure 2i). The similar dissolution process is also observed on the Si substrates. Figure 2, parts d,e and parts g,h correspond to the ZnO nanorods grown on the Si substrates for 3 and 6 h, respectively. When the reaction time increases from 3 to 6 h, the single ZnO nanotower is selectively dissolved from its top to form the volcano-like ZnO nanostructures. It is interesting that the volcano-like (Figure 2g,h) and tube-like (Figure 2i) ZnO nanostructures have the well-faceted side surfaces and a hexagonal cross section. This may be related to the hexagonal wurtzite structure of the ZnO material.

Sun et al. have recently reported that the ZnO nanotubes with diameters in the range of 20−40 nm and the wall thickness of ~7 nm were obtained on the substrate by premixing the reaction solution for 24 h at 90 °C.[21] Without the premixing process, only the ZnO nanorods could be obtained for the same deposition time. Although the growth mechanism of the nanotubes is not further discussed, their experimental results may imply that the reaction time is crucial for the formation of the tubular structure. During the long premixing time (24 h) in Sun's experiment and the longer reaction time in our experiments, the zinc species in the solution can be largely consumed. In this case, the Ostwald ripening will become appreciable and the thermodynamics will dominate the reaction process.[12] The morphology of the ZnO nanostructures will be directed to lower the system energy. The hollow structure may have a lower energy than that of the solid structure due to the higher energy at the polar surfaces.[22] This may facilitate the formation of the ZnO nanovolcanoes and nanotubes.

Obviously, the ZnO powders collected in the reaction solution (Figure 2f) and the ZnO nanostructures obtained on the bare substrates (Figure 2, parts a,b and parts d,e) have different sizes. The nucleation between ZnO crystal and the substrate is ascribed to heteronucleation, while the nucleation of ZnO crystal in solution is ascribed to homogeneous nucleation. The substrates can decrease the free-energy barrier for the formation of crystal nuclei, and heteronucleation takes place at a lower saturation ratio onto a substrate than in solution,[10] which make ZnO nucleate more easily and earlier on the substrate. Therefore, the

effective reaction time of the obtained ZnO nanostructures, that is, the time including the nucleation and growth processes, on the substrates may be longer than that of the ZnO crystal in the solution. As a result, the ZnO nanostructures obtained on the substrates possess larger size than those obtained in the solution in our experiments. Sun et al. also observed that the different ZnO nanostructures, that is, ZnO nanorods and nanotubes, were, respectively, produced in the reaction solution and on the substrate.[21] Similarly, the ZnO nanostructures grown on the substrate may experience a longer reaction process including nucleation and growth, which may result in only the nanotubes obtained on the substrates in Sun's experiment.

Seeds. Vayssiers et al. have reported that the seeds had a weak effect on the morphology of ZnO nanostructures.[11] However, our experimental results show that the morphology and size of ZnO nanostructures is obviously different between the bare substrates and seed-coated substrates. As shown in Figure 2, parts a,b and parts d,e, the ZnO nanostructures grown on the bare ITO and Si substrates are 2−7 μm in length and ∼600 nm in width. Only a few ZnO nanotowers or ZnO nanobundles can be observed on the bare ITO and Si substrates. When the ZnO seed layers are introduced, the dense-arrayed, regular oriented ZnO nanorods can be obtained, as shown in Figure 3a−d. This indicates that the seed layer can facilitate the growth of ZnO nanostructures on the substrates. The seed layer plays three primary roles as follows. First, the growth of the ZnO nanostructure on the ZnO seed layer acts as homoepitaxy. Introducing the seed layer can effectively lower the interface energy between the crystal nuclei and the substrate and hence decrease the nucleation barrier. Second, abundant crystalline interfaces between seeds, which have the fairly high energy, tend to absorb particles or nuclei to lower the system energy. Accordingly, the presence of interfaces can facilitate the growth of the ZnO nanostructures. Third, the ZnO seed layer can increase the surface roughness. The rougher the surface is, the more vacancies that exist at the surface of the substrate where they can absorb and receive atoms, particles, and nuclei. This suggests that the rough surface can also promote the growth of ZnO nanostructures.

Although the seeds are deposited by the electron beam evaporation in the same condition, the difference in the base substrates results in the different seeds formed on the substrates. Therefore, different ZnO nanorod arrays are obtained. As shown in Figure 3a−d, the ZnO nanorods grown on the seed-coated ITO substrate (∼50 nm in width and ∼800 nm in length) have a smaller width and longer length than those grown on the seed-coated Si substrate (∼70 nm in width and ∼250 nm in length). Figure 4 gives the AFM images and XRD spectra of the ZnO seeds on the two different base substrates, respectively. The mean roughness on Si and ITO substrates are 4.4 and 6.7 nm, respectively. On the ITO substrate, the ZnO seeds have the smaller size, and the seed layer has the larger roughness. This may be responsible for the difference of the ZnO nanorods grown on the two different substrates. The greater number of interfaces and vacancies on the ZnO-seed-coated ITO substrate not only can provide more nucleus sites but also make the growth occur more easily. As a result, the higher-density and longer ZnO nanorods can be obtained on the ZnO-seed-coated ITO substrate. In Figure 4b,d, the XRD spectra of the ZnO seeds show the preferred (002) orientation, which suggests the surface is zinc- or oxygen-terminated.[23] Owing to the positive and negative ionic charges on the zinc- and oxygen-terminated ±-(0001) surfaces, respectively, oxygen and zinc ions are easily adsorbed alternately on the surface by electrostatic force to form

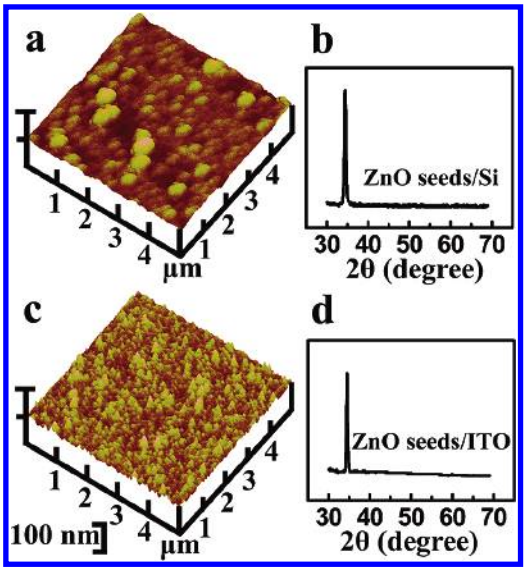

Figure 4. AFM images and XRD spectra of ZnO seeds on (a,b) Si and (c,d) ITO substrates.

(002)-oriented ZnO nanorods. This may promote the preferred growth of the ZnO nanorod arrays along the *c*-axis direction. In addition, the rough surface on the substrate has a high surface energy. It easily adsorbs the high-energy surfaces of ZnO, that is, ±(0001) surfaces, to decrease the surface energy of the substrate and the ZnO nanostructures. This may also promote the preferred growth of ZnO nanorod arrays.

Conclusion

Various ZnO nanostructures, including nanotowers, nanorods, nanovolcanoes, nanotubes, and nanoflowers, have been obtained by the hydrothermal technique. The individual tower-like, tube-like, and volcano-like structures show the perfect hexagonal cross section. The influence of the seeds and the reaction time on the morphology of the ZnO nanostructures is shown. The growth process and growth mechanism are also discussed. Results show that, with the increasing reaction time, the polar surface will be dissolved from its top to form the hexagonal volcano-like and tube-like ZnO nanostructures. The interface energy and surface roughness will remarkably affect the nucleation of ZnO on the substrates and thus further affect the morphology and size of ZnO nanostructures.

References and Notes

(1) Gorla, C. R.; Emanetoglu, N. W.; Liang, S.; Mayo, W. E.; Lu, Y.; Wraback, M.; Shen, H. *J. Appl. Phys.* **1999**, *85*, 2595.
(2) Dietl, T.; Ohno, H.; Matsukura, F.; Cibert, J.; Ferrand, D. *Science* **2000**, *287*, 1019.
(3) Fan, Z.; Lu, J. G. *J. Nanosci. Nanotech.* **2005**, *5*, 1561.
(4) Law, M.; Sirbuly, D. J.; Johnson, J. C.; Goldberger, J.; Saykally, R. J.; Yang, P. *Science* **2004**, *305*, 1269.
(5) Li, Y.; Meng, G. W.; Zhang, L. D.; Phillipp, F. *Appl. Phys. Lett.* **2000**, *76*, 2011.
(6) Kong, X.; Ding, Y.; Wang, Z. *J. Phys. Chem. B* **2004**, *108*, 570.
(7) Han, X.; Wang, G.; Jie, J.; Choy, W.; Luo, Y.; Yuk, T.; Hou, J. *J. Phys. Chem. B* **2005**, *109*, 2733.
(8) Greene, L. E.; Law, M.; Goldberger, J.; Kim, F.; Johnson, J. C.; Zhang, Y. F.; Saykally, R. J.; Yang, P. *Angew. Chem., Int. Ed.* **2003**, *42*, 3031.
(9) Henley, S. J.; Ashfold, M. N. R.; Nicholls, D. P.; Wheatley, P.; Cherns, D. *Appl. Phys. A* **2004**, *79*, 1169.
(10) Vayssieres, L.; Keis, K.; Lindquist, S.; Hagfeldt, A. *J. Phys. Chem. B* **2001**, *105*, 3350.
(11) Vayssiers, L. *Adv. Mater.* **2003**, *15*, 464.
(12) Liu, B.; Zeng, H. *Langmuir* **2004**, *20*, 4196.
(13) Huang, M. H.; Mao, S.; Feick, H.; Yan, H. Q.; Wu, Y. Y.; Kind, H.; Weber, E.; Russo, R.; Yang, P. *Science* **2001**, *292*, 1897.

(14) Greene, L. E.; Law, M.; Tan, D. H.; Montano, M.; Goldberger, J.; Somorjai, G.; Yang, P. *Nano Lett.* **2005**, *5*, 1231.
(15) Wang, Z. L.; Song, J. H. *Science* **2006**, *312*, 242.
(16) Law, M.; Greene, L. E.; Johnson, J. C.; Saykally, R.; Yang, P. *Nat. Mater.* **2005**, *4*, 455.
(17) Lin, Y. R.; Tseng, Y. K.; Yang, S. S.; Wu, S. T.; Hsu, C. L.; Chang, S. J. *Cryst. Growth Des.* **2005**, *5*, 579.
(18) Tong, Y.; Liu, Y.; Shao, C.; Liu, Y.; Xu, C.; Zhang, J.; Lu, Y.; Shen, D.; Fan, X. *J. Phys. Chem. B* **2006**, *110*, 14714.
(19) Zheng, S.; Tong, M.; Chen, X. *Coord. Chem. Rev.* **2003**, *246*, 185.
(20) Wang, Z.; Qian, X.; Yin, J.; Zhu, Z. *Langmuir* **2004**, *20*, 3441.
(21) Sun, Y.; Fuge, G. M.; Fox, N. A.; Riley, D. J.; Ashfold, M. N. R. *Adv. Mater.* **2005**, *17*, 2477.
(22) Yu, H.; Zhang, Z.; Han, M.; Hao, X.; Zhu, F. *J. Am. Chem. Soc.* **2005**, *127*, 2378.
(23) Kong, X. Y.; Wang, Z. L. *Appl. Phys. Lett.* **2004**, *84*, 975.